Gold Bull (2011) 44:3–13
DOI 10.1007/s13404-010-0002-5

TOPICAL REVIEW

Unexpected magnetism in gold nanostructures: making gold even more attractive

Simon Trudel

Published online: 1 February 2011

Abstract Gold nanostructures have attracted widespread attention due to their novel optical, electronic, and biocompatible properties. These make gold nanostructures (and in particular nanoparticles) very attractive for a variety of applications, including catalysis, therapeutics, diagnostics, sensing, and nanoelectronics. In this topical review, the newly discovered magnetic properties of gold nanostructures are highlighted. This unexpected magnetism in gold nanoparticles is a result of (1) the predominant effect of surfaces at the nanoscale, (2) the electronic modification to gold from strongly capping molecules, and (3) the strong spin–orbit coupling of gold. This review discusses the salient experimental results, a theoretical model, and closes by highlighting possible industrial applications of magnetic gold nanostructures.

Keywords Capping molecules · Gold nanoparticles and thin films · Unconventional magnetism · Self-assembled monolayers

Introduction

Nanoscience is attracting considerable attention, in particular in light of emerging useful and intriguing properties that are present in finely divided materials, but absent in their bulk counterpart. Ever since the pioneering work of Brust [1], gold (Au) nanoparticles have been a focus of interest due to their novel optical, electronic, catalytic, sensing, and biomedical applications [2–8]. The development of gold nanoparticle synthesis has led to a renaissance of gold chemistry [9]. A striking example is the dark red color of solutions of gold nanoparticles, which is due to the surface plasmon resonance of the nanoparticles. Surface plasmon resonance is a result of collective oscillations of the electron cloud in a nanoparticle which arises from interaction with light [10–13]. It presents itself as a strong extinction of light in the visible range (~520 nm) and is responsible for the strong red color of gold nanoparticle solutions. This property of colloidal gold probably makes it the longest used form of nanotechnology, where it was used as early as the fourth century of the common era to decorate the Lycurgus Cup (exposed at the British Museum, London), to make stained glass, and as a pigment in the decoration of porcelain [14, 15].

Magnetism is a field where many nanoscale effects abound, resulting either from the reduced size of the material or the predominant effect of surfaces. One of the more surprising recent incarnations of such novel magnetic behavior is the observation of magnetic properties in nanoscaled materials which are diamagnetic (i.e., non-magnetic) in the bulk. This type of behavior has been observed in metal oxide nanoparticles and nanocrystalline films [16, 17], as well as typically paramagnetic (e.g., Pd [18–23]) and diamagnetic (Cu, Ag, Pt [24, 25]) metal nanostructures. The latter include gold-based nanostructures, which will be the topic of this review.

The magnetic properties of the ferromagnetic metals (Fe, Co, and Ni) are a result of the electronic configuration of the 3*d* energy levels. An imbalance of spin-UP and spin-DOWN 3*d* electron population (due to the exchange interaction) leads to unpaired electrons and a net magnetic moment [26, 27]. Magnetism in gold is completely unexpected, as even though its formal gas-phase atomic electronic configuration is [Xenon]$4f^{14}5d^{10}6(sp)^1$ and has

S. Trudel (✉)
Department of Chemistry, University of Calgary,
2500 University Drive NW,
Calgary, AB T2N 1N4, Canada
e-mail: trudels@ucalgary.ca

an unequal number of spin-UP and DOWN electrons, the band structure of gold and its computed density of states reveal gold has a balanced number of spin-UP and DOWN electrons, and is thus diamagnetic [28, 29]. This predicted diamagnetism is in agreement with the experimentally observed negative susceptibility and diamagnetism of bulk gold [30]. Not surprisingly, this unexpected new phenomenon is attracting considerable attention. As it will be made clear in this review, there is still a wide scatter of results in the literature which, while not necessarily contradictory, makes a comprehensive understanding of this phenomena elusive, and an ongoing task. We hope this review will highlight the need for further systematic and comprehensive studies of these gold-containing nanomaterials.

This review will focus on the experimental, and to a lesser extent, theoretical, status of research on the magnetism of gold thin films and nanoparticles. A key common denominator to the observation of magnetism in nanoscale gold, be it as thin films or nanoparticles, is the effect surface-bound molecules play. As such, this review starts with a brief overview of foundation work concerned with the effect surface-capping molecules and self-assembled monolayers have on Au thin films and nanoparticles. We then highlight experimental results showing the magnetic properties of Au nanostructures. In particular, we will emphasize important control studies that contribute to confirm the observed magnetic properties are indeed inherent to the gold nanomaterials, and not parasitic magnetic impurities. A comprehensive model explaining several key features of the experimentally observed behaviors will be presented. We finish off by showing new directions research is taking in this new and fascinating area.

Setting the stage

As was mentioned above, bulk gold is a metallic material, whose 5*d* electrons are buried a few electronvolts below the Fermi level. Hence, these bands are fully occupied, neglecting the small amount of hybridization with the *s* and *p* orbitals [28, 29]. This leads to the diamagnetic properties of bulk gold, which has a magnetic susceptibility χ_d (defined as the magnetization M divided by the applied magnetic field strength H such that $M=\chi_d H$) of -1.42×10^{-7} emu g^{-1} Oe^{-1} [30]. The filling of the 5*d* bands can be experimentally assessed by using X-ray absorption near-edge structure (XANES) spectroscopy. When using hard X-rays, $2p_{1/2}\rightarrow 5d_{3/2}$ and $2p_{3/2}\rightarrow 5d_{3/2,5/2}$ dipole transitions (also called the L_2 and L_3 edges, respectively) can be probed. The measured intensities of the white line transitions are directly proportional to the density of unoccupied 5*d* states (i.e. the number of holes in the 5*d* band) [26, 27]. For bulk gold, these intensities are very low, as the 5*d* bands are nominally full, as explained above. The low intensities result from the small population of 5*d* holes resulting from *s-p-d* hybridization [31]. We will see below that XANES spectroscopy at the Au $L_{2,3}$ edges has been widely used to probe the electronic properties of gold in the context of surface-modified Au nanomaterials, and assess charge redistribution.

Self-assembled monolayers (SAMs) are well-known chemical modifiers enabling tuning of the surface properties of a material [32]. SAMs provide a convenient chemical handle for further chemical modification [33], tune the wetting properties of surfaces [34], and provide an avenue to nanoscale patterning when combined with soft lithographic methods [35, 36]. When bound to the surface of nanocrystals, the SAM can impart solubility, enabling wet chemical processing and reactions to be carried out at the surface [1]. Thiol molecules avidly bind to gold [32], forming a strong $Au^{\delta+}$–$S^{\delta-}$ bond where the partial charges δ are used to illustrate a charge transfer from gold to the sulfur (S) atom.

The synthesis of thiol-capped nanoparticles took flight with Brust's phase transfer method [1], which is still widely used today. As mentioned above, the white line intensity of the XANES Au $L_{2,3}$ edges is proportional to the number of holes in the 5*d* bands. Zhang and Sham have compared the XANES $L_{2,3}$ spectra of pristine gold foils and thiol-capped gold nanoparticles and reported that as the nanoparticle size decreased, the white line intensity was seen to increase [31, 37]. That is to say, more holes are present on the gold atoms of thiol-capped particles, compared to the bulk, as a result of the Au to S charge redistribution. X-ray photoelectron spectroscopy corroborates this behavior and suggests the localized character of these unoccupied Au 5*d* states [31]. As such, the presence of a SAM at the surface of a nanostructure can also be used to modify the electronic properties of the underlying metal.

Two prime examples of this are the effect adsorbed thiol molecules have on the work function Φ and the surface plasmon resonance (*vide supra*) of a material. The change in work function is attributed to the occurrence of a surface dipole, which itself stems from the intrinsic dipole moment of the capping molecule, as well as the charge transfer at the surface [38]. Garcia and co-workers offered an interesting study of how the presence of various capping molecules strongly affects the surface plasmon resonance of gold nanoparticles [39]. The width of the resonance peaks (as measured in absorbance measurements) is inversely proportional to the size of the nanoparticle. For small nanoparticles, one needs to consider the golden body of the capped nanoparticles as an effective core–shell nanostructure, where the core is metallic, and the shell is insulating (see Fig. 1). The thickness of this insulating shell is related

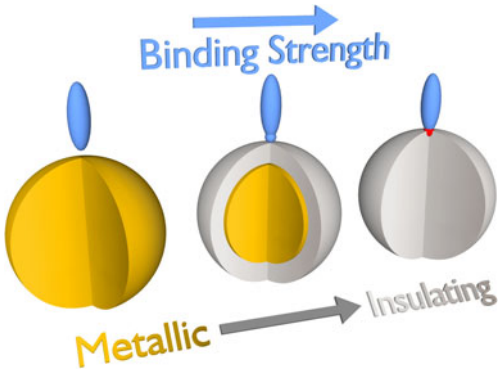

Fig. 1 Formation of electronic core–shell nanostructures due to a surface-capping molecule. From left to right, the binding strength and degree of Au–S charge transfer increases. At the same time, the gold body is seen to go from consisting of only metallic character to a metallic/insulating core–shell, to a fully insulating material

to the strength of Au–S charge transfer at the surface, which localizes the electrons. Strong charge transfer (such as what occurs when thiols are surface-bound) localizes surface conduction electrons, effectively decreasing the size of the metallic core, thereby broadening the surface plasmon resonance peak. For small particles with strongly bound thiols, this insulating shell can become comparable or equal to the total radius of the nanoparticle (see Fig. 1, right), and the breadth of the peak is such that the surface plasmon resonance is suppressed due to the localized character of the electronic charges [39]. Particles coated with a non-binding surfactant such as an ammonium tetraalkyl halide do not create such an insulating layer (Fig. 1, left), and surface plasmon resonance is clearly observed. As will be discussed below, the absence of surface plasmon resonance has been reported to correlate with the onset of magnetism in Au nanoparticles.

Experimental studies

While bulk gold is diamagnetic, there is now a growing and increasingly convincing body of work that shows that magnetic properties can be imparted to nanoscaled gold. This section will highlight studies of magnetism in gold nanoparticles [19, 24, 40–62] and thin films [63–68].

The earliest work was presented by Hori and co-workers [19], who reported on large low-temperature (4.2 K) magnetic moments of 22 μ_B in ~3 nm Au nanoparticles embedded in poly(*N*-vinyl-2-pyrrolidone) (PVP). The anhysteretic magnetization vs. field loop was interpreted in the context of superparamagnetism. This magnetic phase can be explained in terms of coupled spins which are fluctuating due to the randomizing effect of temperature [16, 17, 69]. This work pointedly highlighted the remarkable difference nanoscale gold may have with the bulk state, most noticeably by highlighting the presence of unpaired coupled magnetic moments. Further early studies of the Au–polyvinyl pyrrolidone (PVP) system looked at the size dependence of the saturation magnetization [55], which showed a maximal value around 3 nm over the 1–8-nm diameter range. However, this analysis of the size dependence, in particular of the surface magnetization, has recently come under criticism [70]. A re-interpretation by He shows an increasing and leveling of surface magnetization [70], instead of the declining surface magnetization with increasing particle diameter reported by Hori [55]. Hori and co-workers also investigated dodecanethiol ($CH_3(CH_2)_{11}SH$)-capped Au nanoparticles, but found greatly reduced saturation magnetizations compared to Au–PVP. Further studies conducted by Yamamoto et al. supported the paramagnetic character of small Au nanoparticles, in this case coated with poly (allylamine hydrochloride) (PAAHC) [61]. In this paper, Yamamoto et al. infer that weakly binding capping molecules, such as polymers, are a prerequisite for the observation of magnetic properties in Au nanoparticles.

However, the situation was drastically changed with the publication of the widely cited study by Crespo et al. [40], the most salient feature being shown in Fig. 2a. This figure shows the magnetization vs. field loops measured at room (300 K) and low (5 K) temperature for dodecanethiol-capped Au nanoparticles 1.4 nm in diameter. The characteristic features of a ferromagnetic material, namely a hysteretic behavior with a coercive field and permanent magnetization even in zero applied field, are clearly seen for both temperatures. As a comparison, the corresponding measurements for ~1.5 nm Au nanoparticles with tetraoctylammonium bromide ($((C_8H_{17})_4\ N^+Br$), a weak interacting and non-surface-binding surfactant, are presented in Fig. 2b labelled Au-NR. The dominating behavior is diamagnetic (as seen by the negative slope of the results), and anhysteretic. Only a weak response to the applied magnetic field (as seen by the small magnetization, note the vertical scale is ~3 orders of magnitude smaller in Fig. 2b then in Fig. 2a), more akin to the behavior of bulk gold, is seen. Clearly, the surface decoration is a crucial attribute towards endowing the Au nanoparticles with magnetic properties. It is interesting to compare the optical properties of these two systems, as is shown in Fig. 2c. The thiol-coated nanoparticles do not present surface plasmon resonance while this feature is clearly observed for the ammonium-coated nanoparticles. Crespo and co-workers attribute the magnetic properties to the localized character of the electrons highlighted by the absence of surface plasmon resonance arising due to the strong Au–S charge transfer occurring at the gold–thiolate interface (see ref. [39] and related discussion above). This is in direct contradiction to Yamomoto et al. [61], whereas Crespo found that a strongly binding capping molecule is necessary to observe magnetism.

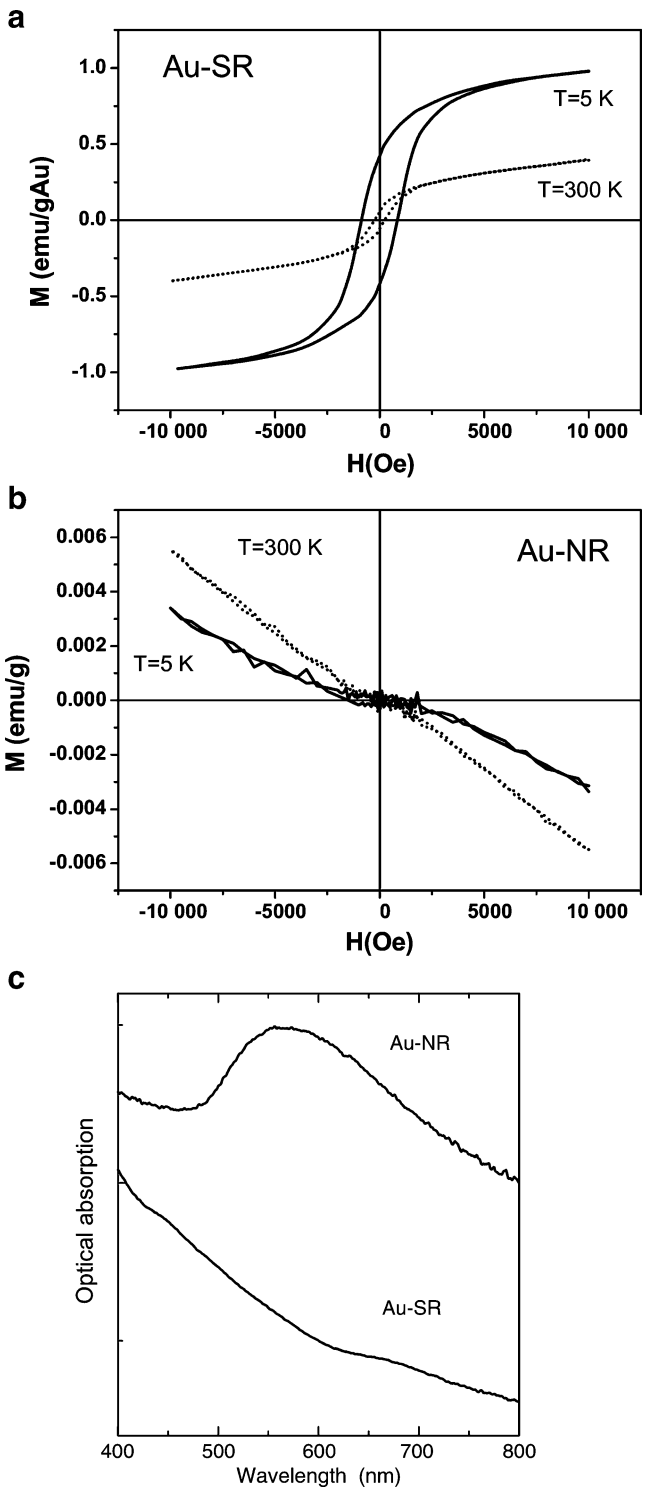

◀ **Fig. 2** Hysteresis loops corresponding to 1.4 nm diameter thiol-capped gold nanoparticles, Au–SR (**a**), and magnetization curves of 1.5–5.0 nm gold nanoparticles stabilized by means of an ammonium surfactant, Au–NR (**b**), at 5 and 300 K. For the Au–SR sample, the magnetization is given in electromagnetic units per gram of gold. UV-visible absorption spectra for the two studied gold nanoparticles (**c**). The strong surface plasmon resonance band around 550 nm, observed for the Au–NR sample, is absent in the case of Au–SR. Reprinted figure with permission from Crespo, Litrán, Rojas, Multigner, de la Fuente, Sánchez-López, García, Hernando, Penadés, and Fernández (2004) Phys Rev Lett 93:087204. Copyright 2010 by the American Physical Society

The magnetic properties of nanoscaled materials are well-known to be temperature dependent. When thermal energy is sufficient to overcome the energy barrier that maintains the magnetic moments along a given direction, the particle becomes superparamagnetic and the particle's large moment fluctuates [16, 17, 69]. This barrier is known as the anisotropy energy barrier and is proportional to the product of the anisotropy constant K and the volume V of the nanoparticle. The blocking temperature T_B is the temperature below which the energy barrier is not overcome, and the particle's moment is said to be blocked. Below the blocking temperature, hysteretic M vs. H loops are measured, as is shown in Fig. 2a. The anisotropy constant is approximately related to the blocking temperature by

$$K \approx \frac{25 k_B T_B}{V} \quad (1)$$

where k_B is Boltzmann's constant. Given a blocking temperature greater than 300 K and the small diameter of the nanoparticles studied, Crespo approximated the anisotropy constant has a lower-limit value on the order of 7×10^7 J/m^3 [40]. This is a *huge* value, almost a full order of magnitude, more than typical high magnetic anisotropy uniaxial materials such as $SmCo_5$ and FePt. Neglecting shape effects for spherical nanoparticles, the anisotropy constant is a measure of the anisotropy of the spin–orbit coupling interaction due to the directional character of bonding in a solid [26, 27]. For gold nanoparticles, this huge anisotropy constant is then attributed to the anisotropy of the Au–S bond, as well as the large spin–orbit coupling at the Au surface [71].

While there is a clear dichotomy between the nanoscaled ferromagnetic and bulk diamagnetic gold, the clear cutoff between the two behavior is still elusive and requires further attention. Focusing on dodecanethiol-capped nanoparticles, for which room temperature permanent magnetism was observed for particle diameters of 1.4 nm [40], Dutta and collaborators turned their attention to larger particles with diameters of 5 and 12 nm [45]. For the 5-nm nanoparticles, permanent magnetism is observed at 5 K, while a superparamagnetic behavior is seen at room temperature. The blocking temperature is 50 K, pointing to an overall decrease of the anisotropy constant when compared to 1.4 nm particles (to ~3×10^5 J/m^3 when using Eq. 1 above). For 12 nm nanoparticles, only diamagnetic behavior is recorded at all temperatures. As such, the importance of the contribution of surface atoms is highlighted. For the larger particles, the surface atoms do not contribute sufficiently to dictate the magnetic behavior, and the diamagnetic core dominates the measured response.

While the occurrence of magnetism in Au nanoparticle systems is now well established, the obvious question one faces

is whether the observed magnetism is an intrinsic property of the gold. The common method of characterization of gold nanoparticles is superconducting quantum interference device (SQUID) magnetometry, which while very sensitive, is a non-specific tool which cannot discriminate against parasitic secondary magnetic phases and measurement artifacts. It is thus easy to misinterpret the origin of magnetism in a given sample [72–75]. Of particular concern are impurities of iron and its oxides, which form magnetic materials. A common check is the use of inductively coupled plasma mass spectrometry, and indeed most investigations report iron concentrations in the parts per million range, an amount insufficient to account for the observed magnetic responses. Crespo et al. deliberately prepared Fe-doped Au nanoparticles, with Fe atomic percentages of up to 18% [41]. It was shown that the presence of iron actually *lowers* the observed magnetic moments as well as the coercive fields, as the Fe impurities behave as para- or superparamagnetic. While suggesting the magnetic response is not attributable to Fe impurities, this study does not directly prove it is intrinsic to gold.

A first element-specific proof of a magnetic moment on gold was provided by Yamamoto et al. during their study of PAAHC–Au nanoparticles highlighted above, using X-ray magnetic circular dichroism (XMCD) [61]. This method consists of measuring $L_{2,3}$ absorption edges using circularly polarized X-ray photons, in the presence of a magnetic field which is applied along and against the X-ray photon's momentum. The difference between the two XANES spectra yields the XMCD spectrum. This technique probes the difference between spin-UP and spin-DOWN densities of states [27]. The measured Au L_3 edge XANES and XMCD spectra are presented in Fig. 3 for 1.9 nm PAAHC-coated gold nanoparticles in a 10-T magnetic field. The peaks in the XMCD spectrum confirm that Au atoms are bearing a magnetic moment. The XMCD data also tracks the SQUID magnetometry results, strongly supporting the observed magnetic properties are due to the gold, and not parasitic magnetic impurities. In addition to PAAHC–Au nanoparticles [61, 76], this method was also used to confirm the magnetic character of dodecanethiol-capped Au nanoparticles [24, 52], as is shown in Fig. 4a. Here, the field dependence of the magnetization extracted from the amplitude of the XMCD signal is shown. The measurement shows a clear hysteresis as SQUID-measured M vs. H loops did [24]. To complement the XMCD measurements, ^{197}Au Mössbauer spectroscopy [77] was performed on these nanoparticles [24]. The spectrum measured at 4.2 K is shown in Fig. 14b. In addition to the non-magnetic singlet attributed to the core diamagnetic gold atoms, a magnetically split signal is also observed, which is attributed to the surface magnetic gold atoms. As with XMCD, this is clear evidence of gold-born magnetic moments. The muon spin resonance technique also provides a microscopic, if not element-specific probe to the magnetic environment.

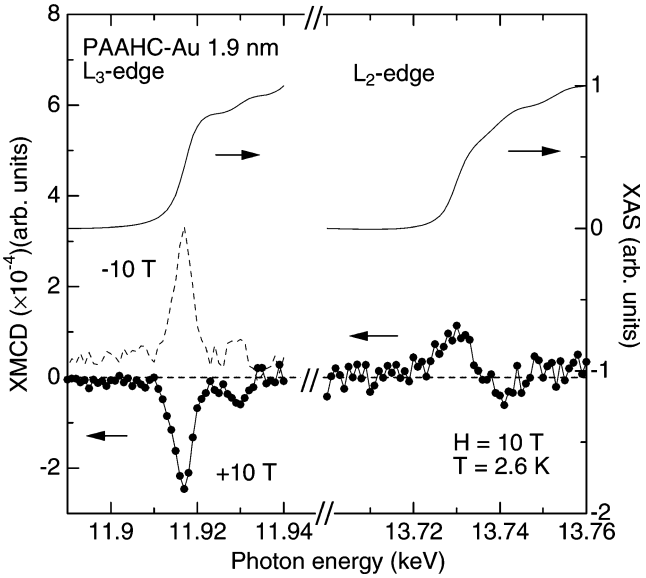

Fig. 3 XMCD and X-ray absorption spectroscopy (XAS) spectra at the Au L_3 and L_2 edge with an applied magnetic field of 10 T. The XMCD and XAS spectra include a same scale factor so that the height of the edge jumps off the XAS spectra (*solid lines*) are unity. *Solid lines with closed circle* symbols represent an XMCD spectrum with an applied magnetic field of 10 T, while the *dotted line* indicates an XMCD spectrum in a magnetic field applied in the opposite direction, implying the observed signal is not an artificial effect. Reprinted figure with permission from Yamamoto, Miura, Suzuki, Kawamura, Miyagawa, Nakamura, Kobayashi, Teranishi, and Hori (2004) Phys Rev Lett 93:116801. Copyright 2010 by the American Physical Society

Goikolea and colleagues have shown the presence of a dipolar field consistent with long-range magnetic ordering in 2.1 nm dodecanthiol-capped Au nanoparticles [49].

In addition to polymer-encapsulated [19, 54, 55, 60, 61, 78] and alkanethiol-coated nanoparticles [24, 40, 44–49, 51–53], magnetism has now been observed in Au nanoparticles coated with ligands such as thiolated sugars [41, 42] and biomolecules [48, 51], thiolated azobenzenes [58, 59], phosphine [53], and oleic acid and/or oleic amine [43, 57]. The behaviors range from permanent, ferromagnetic-like at room temperature, to superparamagnetic, to paramagnetic. In addition to undesired impurities, the effect of nanoparticle size and distribution, as well as chemical identity, surface binding strength, and packing density of the capping ligands must be taken into consideration to undertake a comprehensive and thorough comparison of all the studied systems, which is beyond the scope of the present review. In addition, the observed saturation magnetization spans a wide range, from as low as 0.01 to 5 emu/g Au [24, 52]. This latter value corresponds to a magnetic moment of 0.33 μ_B per surface Au atom. This very high value is comparable to the moment of bulk Ni of 0.606 μ_B/atom [79].

While we have up to now focused on Au nanoparticles, magnetic properties can also be imparted to thin films [63–

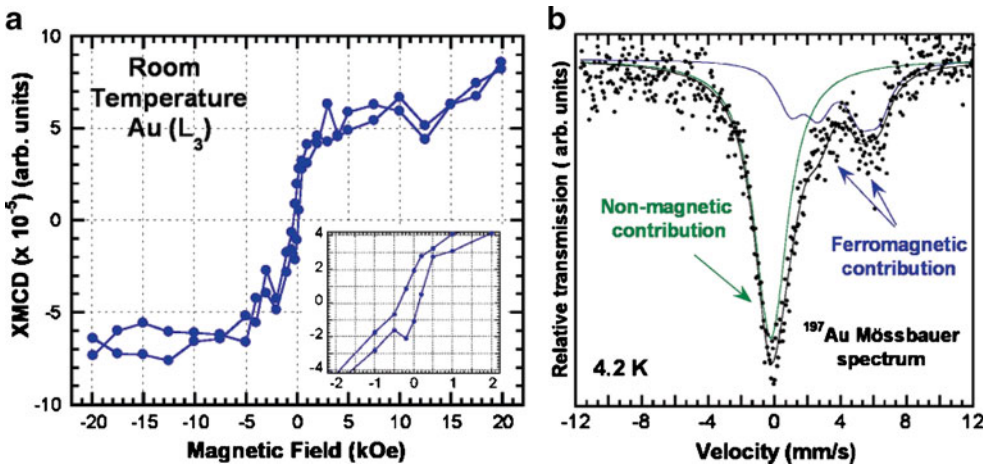

Fig. 4 **a** Element-specific magnetization of dodecanothiol-capped Au nanoparticles obtained from the amplitude of the XMCD spectra at the Au L_3 edge as a function of the applied magnetic field. The coercivity of the element-specific magnetization is clearly observed in the *inset*. **b** ^{197}Au Mössbauer spectrum of dodecanothiol-capped Au nanoparticles at 4.2 K. The spectrum has been fitted by a non-magnetic singlet contribution corresponding to the inner Au atoms with an *fcc* structure and a ferromagnetic one from the surface Au atoms. Reprinted with permission from [24]

68]. The main results can be summarized as follows. Firstly, the magnetic properties are highly anisotropic, as magnetization is only observed when the magnetic field is applied perpendicular to the thin film's plane, i.e., along the general orientation of the Au–S and hydrocarbon chain when considering an alkanethiol SAM [63, 66, 68]. An example is shown in Fig. 5 where M vs H loops were measured for a Au thin film coated with a photochromic azobenzene SAM [68]. This points to a large perpendicular magnetic anisotropy constant, as demagnetization effects tend to coerce the magnetization within the sample plane. Secondly, considering there are on the order of 2×10^{14} atoms per centimeter squared on the Au(111) surface, one can estimate the magnetic moment per surface atom. For the measurements presented in Fig. 5, this corresponds to approximately 50 μ_B per surface Au atom. This is an extraordinarily giant moment, and moments up to 100 μ_B per surface Au have been reported [66]. Thirdly, despite the very strong anisotropy and large moment, no or very small hysteresis is observed, as the sample exhibit paramagnetism. A final effect that was seen to occur is related to the aging of samples exposed to air [63, 64]. Over a period of almost 2 weeks, the saturation magnetization of poly(analine) SAMs on gold was more than halved. It is interesting to note that this effect has not been specifically addressed for gold nanoparticles, and could (in part) account for the scatter in reported magnetic moments.

Model of FM in Au: thin films vs. nanoparticles

The development of an inclusive theoretical model which takes into account the wide range of experimental results for both thin films and nanoparticles is a daunting task. To summarize what has been presented up to now, such a model should describe the large anisotropies seen in both nanoparticles and thin films, explain the discrepancy in magnetic moments between nanoparticles (on the order of ~0.01 μ_B) and thin films (50~100 μ_B), and finally explain why hysteresis is observed in nanoparticles, while paramagnetic-like, anhysteretic M vs. H loops are seen in thin films. Here, we will describe the model put forth by Hernando and co-workers [66, 80], as it is rather comprehensive and widely cited. Readers interested in other models are directed to the primary literature [81–85].

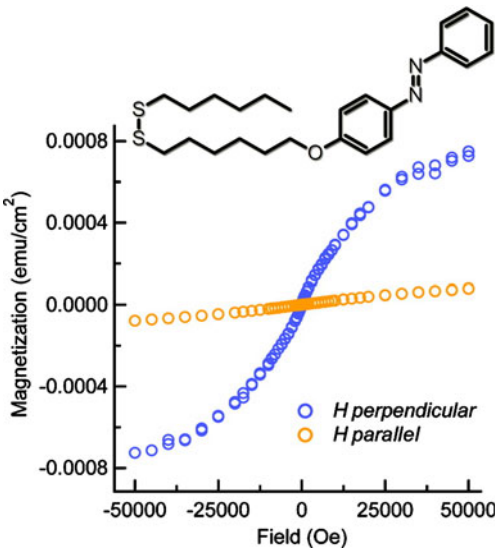

Fig. 5 Plots of the magnetization M vs. applied magnetic field H at 5 K for a SAM formed from the disulfide 4-[6-(hexyldithio)hexyloxy] azobenzene (shown) when the external magnetic field was applied perpendicular (*blue points*) and parallel (*orange points*) to the substrate surface. Reprinted with permission from [68]

We begin with the magnetic properties of thin films coated with SAMs. SAMs will form ordered domains [32], which can have dimensions upwards of tens of nanometres [86, 87]. The SAM leads to a modification of the surface potential, with respect to bare Au [38, 59, 68, 88]. In particular, an energy barrier is created at the boundary of such a domain, and the ordered area becomes a potential well where quasi-free surface electrons become captured, as is schematically shown in Fig. 6. The traveling electron in this atomic-like orbital will generate an orbital moment L_z, where z is along the film normal as the electron is confined to travel in the surface plane. It is assumed the domains are circular and of radius ξ.

Hernando and co-workers propose a Hamiltonian describing this situation whose energy can be minimized with respect to angular momentum L_z [89], with the result that L_z is proportional to the domain radius squared (ξ^2) [80]. Given this ξ-dependence of the minimized orbital energy, Hernando et al. clearly show that very large orbital moments may be expected, and are comparable to the moments experimentally observed for thin films. The electrostatic interaction between the electrons is such that their energy is minimized for parallel (i.e., ferromagnetic) spin alignment [84], in a manner analogous to Hund's first rule [26, 27]. This is represented as the arrow labeled "Exchange" in Fig. 6. As the spin–orbit coupling interaction is strong in gold, the alignment of spin momenta implies the alignment of orbital momenta. Such well-characterized angular momenta were reported from electron circular dichroism measurements of Au films coated with chiral poly(alanine) [64].

As Hernando et al. point out [80], this model is in agreement with several experimental observations. The electrons responsible for the magnetism are trapped and thus have reduced mobility, which explains the suppression of the surface plasmon resonance as explained above [39, 40]. The orbital moment will be larger for larger well-ordered domains within the SAMs. The aging of the magnetic properties [63, 64] can thus be interpreted as a size reduction of these domains over time. Finally and importantly, while this model predicts large orbital momenta in large domains, as can be obtained in thin films, it also predicts small moments for small domains. This situation would correspond to nanoparticles, where well-ordered SAM domains are tightly limited by the crystalline facets of the particle. As such, only very small moments are observed for nanoparticles. While in principle larger moments would thus be expected for larger particles, this is counterbalanced by core diamagnetism, as volume increases faster than surface as the particle size increases [15].

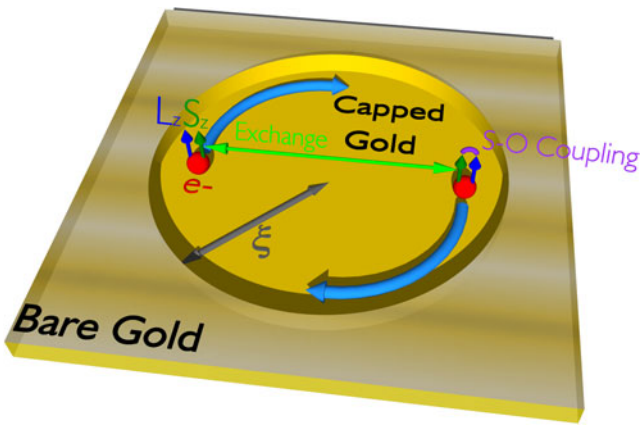

Fig. 6 Quasi-free electrons trapped in an atomic-like orbital resulting from the surface potential of the SAM. The spins of conduction electrons are coupled to minimize electrostatic interactions, and the large orbital momenta are coupling via the spin–orbit coupling interaction

The occurrence of hysteresis is also handled by this model [66]. The spin and orbital momenta of the conduction electrons are coupled, as explained above. When one considers the coupling of these momenta to a localized spin S_Z, the coercive field H_c required for magnetization reversal is inversely proportional to the total coupled moments [90]. For thin films with a large orbital moment L_z, the coercive field vanishes, and no magnetization remains in zero applied field as a vanishing small field is required for magnetization reversal. For small particles, where the orbital moment is very small ($L_z \sim 1$), hysteresis is observed.

New directions

In this section, we will discuss new directions research in this new exciting field is taking.

Our discussion has focused on pristine-capped Au nanoparticles. It was recently reported that ferromagnetism is also observed in $Au_{48}Pt_{52}$ nanowires [91]. In this case, the charge transfer is not believed to occur due to the presence of the capping ligand, but rather occurs internally. While Au has formally filled $5d^{10}$ orbitals, platinum (Pt) has a $5d^9$ electronic configuration. As such, electron density is withdrawn from the gold and relocated on the Pt atom. This is confirmed using XANES spectroscopy by an increase of the Au L_3 edge white line intensity, which is accompanied by a corresponding decrease at the Pt L_3 edge. This is corroborated by comparing with $Au_{25}Pt_{75}$ nanowires, where the Au and Pt L_3 edges were superimposable with the corresponding parent metal foils. In these nanowires where no $5d$ charge relocalization occurred, only paramagnetism was observed. It is worth noting such alloys cannot be obtained in the bulk, where the room temperature solubility of Au in Pt is 4%. This

study suggests novel nanoscaled gold-based alloys can exhibit magnetism.

An indirect demonstration of magnetism in gold thin films was presented by Knaus and co-workers, where the Hall effect in a cobalt–gold bilayer was seen to be modified by capping with dodecanethiol [67]. The changes in the magnetotransport are described as arising from the modified magnetization reversal in the cobalt layer in the presence of a biasing field from the Au–S interface. This new handle on a physical property is expected to contribute to the understanding of the thiol-induced magnetization at the gold surface. Further work on magnetotransport of gold-based nanostructures is expected.

As has been amply discussed above, the Au to S charge transfer is believed to be responsible for the onset of ferromagnetism in thiol-capped gold nanoparticles and thin films. As such, tuning the charge transfer provides a way to tune the magnetic properties. The charge transfer is expected to be influenced by the work function of the metal, which is itself modified by

$$\Delta\Phi = \frac{N \cdot e \cdot \mu \cdot \cos\theta}{\varepsilon_0 \cdot A}$$

due to the presence of the capping molecule [38, 59, 68, 88]. Here, N is the density of dipoles on the surface, μ is the effective dipole moment of the capping molecule (taken to be positive when pointing out of the surface), θ is the average tilt angle of the capping molecule in the SAM, ε_0 is the permittivity of vacuum, and A is the area taken up by a molecule (around 21.4 Å^2 per chain for docosyl mercaptan [$CH_3(CH_2)_{21}SH$] on Au(111) [92]). The presence of the molecule produces a surface dipole, which will raise or lower the vacuum level in the SAM, thereby raising or lowering the lowest unoccupied molecular orbital (LUMO) of the capping molecule with respect to the Fermi level ε_F of the gold, as is shown in Fig. 7. As is illustrated, the energy barrier $\phi_{e\text{-inj}}$ to charge injection from the gold to the molecule (i.e., charge transfer) is also modulated by this surface modification. Whereas, a negative dipole moment (such as in a molecule with an electron withdrawing group) results in a decrease of the work function Φ and charge transfer barrier $\phi_{e\text{-inj}}$, a positive dipole moment increases the metal's work function and charge transfer barrier.

The work function of the gold surface can be reversibly tuned if it is capped with a photochromic molecular switch such as an azobenzene whose surface dipole is reversed upon photoisomerization [93]. The *cis-trans* photoisomerization leads to a reversible modification of the dipole moment of the molecule from positive to negative, and thus reversibly changes the work function of the metal. As such, a modulation of the magnetism is thus expected if gold is coated with a photochromic switch and shined with light of the appropriate wavelength.

This principle was recently demonstrated by Suda and co-workers for gold nanoparticles [58, 59] and thin films [68] coated with thiolated azobenzene photoswitches. In both cases, reversible modulation of the magnetization of ~25% was observed. Figure 8 shows the reversible phototuning of the magnetic properties of azobenzene-coated Au nanoparticles [59]. As can be seen, the magnetization is reversibly changed with successive irradiation with UV and visible light. This type of system is particularly attractive with respect to fundamental studies, as the magnetic properties and their associated properties can be studied while maintaining the nanoparticle size and morphology strictly unchanged.

Remaining issues need to be understood and elucidated, which would hopefully shed some light onto the wide scatter of behaviors observed. In particular, the effects of packing density and the density of defects within the SAM need to be investigated, as both would be expected to modify the dipole moment layer, and thus the Au–S charge injection and resulting magnetism. This particular topic is of interest to our group, and we are currently investigating such topics.

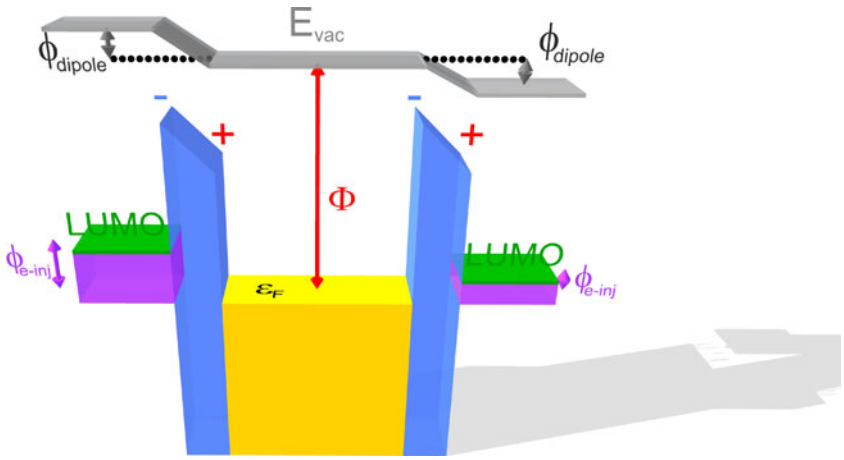

Fig. 7 Schematic representation of the change of the energy barrier to charge transfer $\phi_{e\text{-inj}}$ arising from the modification of the vacuum energy E_{vac} due to surface dipoles ϕ_{dipole}. On the *left*, a positive dipole moment is shown while on the *right* a negative dipole moment is shown. LUMO of the capping molecule, ε_F is the Fermi level of Au, and Φ is the work function of un-capped Au

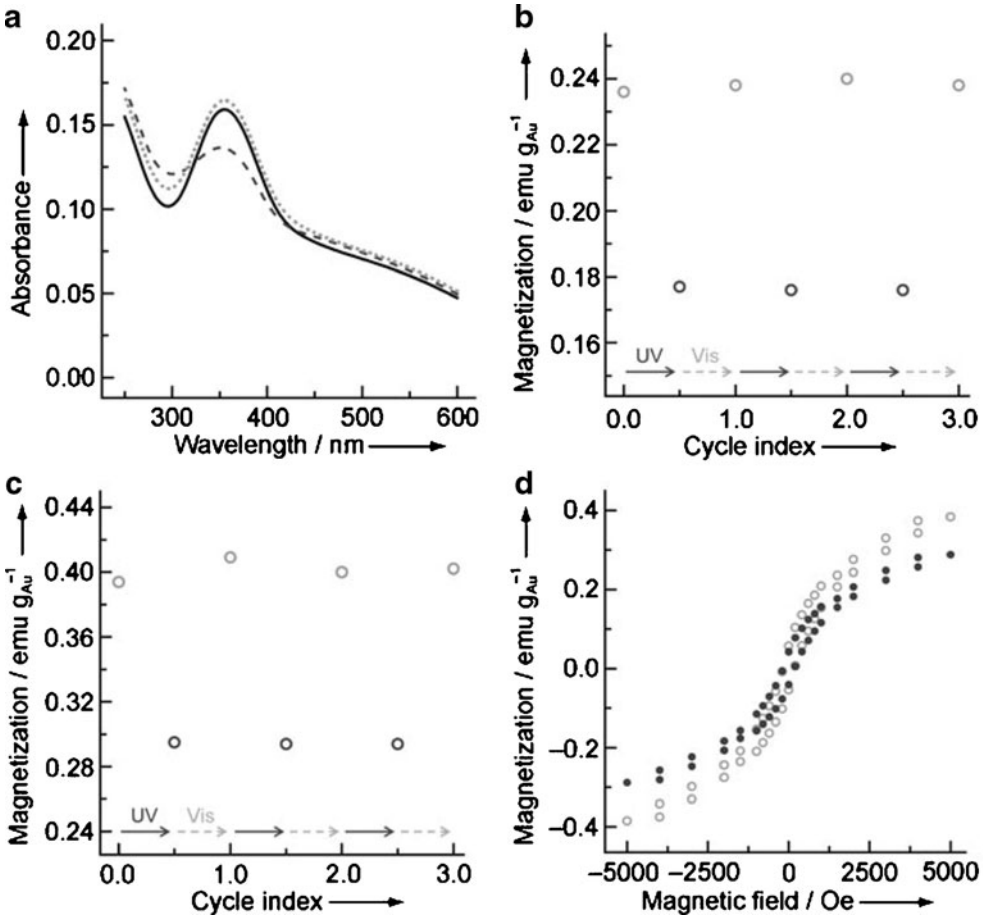

Fig. 8 Changes in the optical properties (**a**), room temperature (**b**) and 5 K (**c**) magnetization, and 5 K magnetization reversal (**d**) as a result of photoisomerization in azobenzene-coated Au nanoparticles. Suda, Kameyama, Suzuki, Kawamura, and Einaga (2008) Reversible phototuning of ferromagnetism at Au–S interfaces at room temperature. Angew Chem Int Ed 47:160–163. Copyright Wiley-VCH Verlag GmbH & Co. KGaA. Reproduced with permission [59]

Outlook to potential industrial applications

In this final section, potential industrial applications wherein magnetic gold nanoparticles could provide a strategic advantage over other materials are discussed. Note that given this field is still burgeoning, none of these applications have yet been demonstrated.

In the short-term, one may expect that the magnetism of Au nanostructures will be coupled to previously known properties of Au. A first niche application would be gold nanoparticle-based catalysis. The magnetic properties could provide the means to recover a catalyst, by applying a magnetic field, which could be used again. This prospect is especially interesting as Bond has recently reviewed that smaller particles reaching the non-magnetic state are more catalytically active [6]. This coincides with the trend towards magnetism for small particles with localized electrons (*vide supra*), and as such magnetism and catalytic properties might inherently go hand in hand. The prospect of magnetism in capping ligand-free Au–Pt nanostructures highlighted in the previous section [91] is especially interesting, as the anticipated competition for the nanoparticle's surface between capping ligand and substrate would be eliminated.

Au nanostructures have already shown their tremendous potential towards diagnostics and therapeutics [2, 3, 8]. Adding magnetism to Au nanoparticles could make them a silver (well, technically, golden) bullet. New functionality towards magnetic resonance imaging and magnetic hyperthermia (which have up to now been the fiefdom of magnetic metal oxide nanoparticles [17]) would considerably enhance the already long list of desirable attributes of gold nanoparticles towards biomedically engineered health solutions. It is anticipated such functionality in gold-based

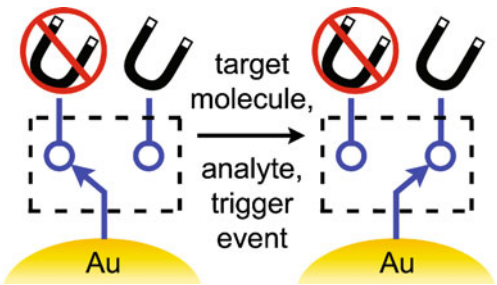

Fig. 9 Schematic representation of switching magnetism from off to on in gold-based nanostructures. The switch may arise due to binding of a target molecule, a chemical reaction at the nanostructure's surface, or irradiation with light of a proper wavelength

nanostructures could be demonstrated in as short a time scale as a couple of years.

Finally, the possibility to chemically turn *on* magnetism in gold nanostructures is a very unique feature. One can envisage how gold nanoparticle-based sensors could be implemented, where the binding or chemical reaction of a surface molecule could lead to the onset of magnetism, as is schematically shown in Fig. 9. Photomagnetic gold nanoparticles (as highlighted in the above section [59]) could be engineered towards obtaining true on–off reversible behavior, instead of a simple modulation of the magnetic moment. However, before this is achieved, a deeper understanding of what chemical surface modifications leads to magnetism is required. However, the prospect of turning magnetism on at will is attractive towards sample enrichment, separation of gold, sensing, as well as a new medium for magnetooptical data storage.

Conclusions

The unexpected magnetism in gold nanostructures presents several standing challenges before we fully understand the physical and chemical handles governing it. However, it also presents new opportunities to test our understanding of the electronic properties of finely divided matter. It also opens new industrial avenues towards the design of new functional materials. Noticeably, applications in catalysis, biomedicine, and information technology can be anticipated as the new properties of these fascinating new gold-based nanomaterials are harnessed. Gold has indeed become even more attractive in its own new special way.

Acknowledgements The University of Calgary is acknowledged for financial support and start-up funds.

References

1. Brust M, Walker M, Bethell D et al (1994) Chem Commun 801
2. Daniel M-C, Astruc D (2004) Chem Rev 104:293
3. Jain PK, Huang X, El-Sayed IH et al (2008) Acc Chem Res 41:1578
4. Rosi NL, Mirkin CA (2005) Chem Rev 105:1547
5. Talapin DV, Lee J-S, Kovalenko MV et al (2010) Chem Rev 110:389
6. Bond G (2010) Gold Bull 43:88
7. Grisel R, Wetstrate K-J, Gluhoi A et al (2002) Gold Bull 35:39
8. Huang X, Neretina S, El-Sayed MA (2009) Adv Mater 21:4880
9. Whyman R (1996) Gold Bull 29:11
10. Link S, El-Sayed MA (2003) Annu Rev Phys Chem 54:331
11. Link S, El-Sayed MA (1999) J Phys Chem B 103:8410
12. Myroshnychenko V, Rodriguez-Fernandez J, Pastoriza-Santos I et al (2008) Chem Soc Rev 37:1792
13. Zhao J, Pinchuk AO, McMahon JM et al (2008) Acc Chem Res 41:1710
14. Wilson R (2008) Chem Soc Rev 37:2028
15. Cortie MB (2004) Gold Bull 37:12
16. Sundaresan A, Rao CNR (2009) Nano Today 4:96
17. Trudel S, Hill RH (2010) Magnetic metal oxide nanocrystals and their applications. In: Umar A, Hahn Y-B (eds) Metal oxide nanostructures and their applications. American Scientific, Valencia, and references therein
18. Hernando A, Sampedro B, Litrán R et al (2006) Nanotechnology 17:1449
19. Hori H, Teranishi T, Nakae Y et al (1999) Phys Lett A 263:406
20. Litrán R, Sampedro B, Rojas TC et al (2006) Phys Rev B 73:054404
21. Sampedro B, Crespo P, Litrán R et al (2003) Phys Rev Lett 91:237203
22. Shinohara T, Sato T, Taniyama T (2003) Phys Rev Lett 91:197201
23. Xiao C, Ding H, Shen C et al (2009) J Phys Chem C 113:13466
24. Garitaonandia JS, Insausti M, Goikolea E et al (2008) Nano Lett 8:661
25. Suber L, Dino F, Scavia G et al (2007) Chem Mater 19:1509
26. Kübler J (2009) Theory of itinerant electron magnetism, Revised edn. Oxford Science Publications, Oxford
27. Stöhr J, Siegmann HC (2006) Magnetism: from fundamentals to nanoscale dynamics. Springer, Heidelberg
28. Ramchandani MG (1970) J Phys C Met Phys 3:S1
29. Sommers CB, Amar H (1969) Phys Rev 188:1117
30. Lide DR (ed) (2009–2010) Handbook of chemistry and physics. CRC Press, Boca-Raton
31. Zhang P, Sham TK (2003) Phys Rev Lett 90:245502
32. Love JC, Estroff LA, Kriebel JK et al (2005) Chem Rev 105:1103
33. Templeton AC, Wuefling WP, Murray RW (2000) Acc Chem Res 33:27
34. Chaudhury MK, Whitesides GM (1992) Science 256:1539
35. Gates BD, Xu Q, Stewart M et al (2005) Chem Rev 105:1171
36. Xia Y, Whitesides GM (1998) Angew Chem Int Ed 37:550
37. Zhang P, Sham TK (2002) Appl Phys Lett 81:736
38. Ray SG, Cohen H, Naaman R et al (2005) J Phys Chem B 109:14064
39. García MA, de la Venta J, Crespo P et al (2005) Phys Rev B 72:241403(R)
40. Crespo P, Litrán R, Rojas TC et al (2004) Phys Rev Lett 93:087204
41. Crespo P, García MA, Pinel EF et al (2006) Phys Rev Lett 97:177203
42. de la Fuente JM, Alcantara D, Eaton P et al (2006) J Phys Chem B 110:13021
43. de la Presa P, Multigner M, de la Venta J et al (2006) J Appl Phys 100:123915
44. de la Venta J, Pucci A, Pinel EF et al (2007) Adv Mater 19:875
45. Dutta P, Pal S, Seehra MS et al (2007) Appl Phys Lett 90:213102
46. Guerrero E, Rojas TC, Multigner M et al (2007) Acta Mater 55:1723
47. Crespo P, García MA, Fernandez-Pinel E et al (2008) Acta Phys Pol A 113:515
48. Crespo P, Guerrero E, Munoz-Marquez MA et al (2008) IEEE Trans Magn 44:2768
49. Goikolea E, Garitaonandia JS, Insausti M et al (2008) J NonCryst Solids 354:5210
50. Guerrero E, Munoz-Marquez MA, Fernandez-Pinel E et al (2008) J Nanopart Res 10:179
51. Guerrero E, Munoz-Marquez MA, García MA et al (2008) Nanotechnology 19:17501

52. Garitaonandia JS, Goikolea E, Insausti M et al (2009) J Appl Phys 105:07A907
53. Guerrero E, Munoz-Marquez MA, Fernandez A et al (2010) J Appl Phys 107:064303
54. Hori H, Teranishi T, Taki M et al (2001) J Magn Magn Mater 226–230:1910
55. Hori H, Yamamoto Y, Iwamoto T et al (2004) Phys Rev B 69:174411
56. Nakae Y, Seino Y, Teranishi T et al (2000) Phys B 284:1758
57. Rueda T, de la Presa P, Hernando A (2007) Solid State Commun 142:676
58. Suda M, Kameyama N, Ikegami A et al (2009) Polyhedron 28:1868
59. Suda M, Kameyama N, Suzuki M et al (2008) Angew Chem Int Ed 47:160–163
60. Yamamoto Y, Hori H (2006) Rev Adv Mater Sci 12:23
61. Yamamoto Y, Miura T, Suzuki M et al (2004) Phys Rev Lett 93:116801
62. Yamamoto Y, Miura T, Teranishi T et al (2004) J Magn Magn Mater 272:E1183
63. Carmeli I, Leitus G, Naaman R et al (2003) J Chem Phys 118:10372
64. Vager Z, Carmeli I, Leitus G et al (2004) J Phys Chem Solids 65:713
65. Reich S, Leitus G, Feldman Y (2006) Appl Phys Lett 88:222502
66. Hernando A, Crespo P, García MA et al (2006) Phys Rev B 74:052403
67. Knaus B, Garzon S, Crawford TM (2009) J Appl Phys 105:07A903
68. Suda M, Kameyama N, Ikegami A et al (2009) J Am Chem Soc 131:865
69. Bean CP, Livingstone JD (1959) J Appl Phys 30:120S
70. He L (2010) Phys Rev B 81:096401
71. LaShell S, McDougall BA, Jensen E (1996) Phys Rev Lett 77:3419
72. Chambers SA, Droubay T, Wang CM et al (2003) Appl Phys Lett 82:1257
73. García MA, Fernandez Pinel E, de la Venta J et al (2009) J Appl Phys 105:013925
74. Lefebvre J, Trudel S, Hill RH et al (2008) Chem Eur J 14:7156
75. Grace PJ, Venkatesan M, Alaria J et al (2009) Adv Mater 21:71
76. Yamamoto Y, Miura T, Teranishi T et al (2006) Phys Rev Lett 96:139902
77. Parish RV (1982) Gold Bull 15:51
78. Mallick K, Witcomb M, Erasmus R et al (2009) J Appl Phys 106:074303
79. Kittel C (1996) Introduction to solid state physics. John Wiley, New York
80. Hernando A, Crespo P, García MA (2006) Phys Rev Lett 96:057206
81. Gonzalez C, Simon-Manso Y, Marquez M et al (2006) J Phys Chem B 110:687
82. Micheal F, Gonzalez C, Mujica V et al (2007) Phys Rev B 76:224409
83. Luo W, Pennycook J, Pantelides ST (2007) Nano Lett 7:3134
84. Vager Z, Naaman R (2004) Phys Rev Lett 92:087205
85. He L (2010) J Phys Chem C 114:12487
86. Barrena E, Ocal C, Salmeron M (1999) J Chem Phys 111:9797
87. Tamada K, Hara M, Sasabe H et al (1997) Langmuir 13:1558
88. Wu DG, Ghabboum J, Martin JML et al (2001) J Phys Chem B 105:12011
89. Specifically, $L_z = m\xi^2\alpha_r s_z$, where s_z is the z-component of the electron's spin, m is the electron mass, and α_r is the energy splitting of p bands resulting from spin-orbit coupling. See ref. 80 for more details
90. Specifically, $H_c = 2K[\mu_0\mu_B(2s_z + 2s_z + L_z)]^{-1}$, where μ_0 is the permeability of vacuum. See ref. 66 for more details
91. Teng X, Feygenson M, Wang Q et al (2009) Nano Lett 9:3177
92. Strong L, Whitesides GM (1988) Langmuir 4:546
93. Qune L, Akiyama H, Nagahiro T et al (2008) Appl Phys Lett 93:083109